1

SIMPLE PREDATOR-PREY INTERACTIONS CONTROL DYNAMICS IN A PLANKTON FOOD WEB MODEL

Roger Cropp[1] and John Norbury[2]

[1] Centre for Environmental Systems Research, Griffith School of Environment, Griffith University, Nathan, Queensland, 4111, Australia.

[2] Mathematical Institute, University of Oxford, 24-29 St Giles, Oxford, OX1 3LB, UK.

ABSTRACT

A plankton food web model is analysed using interaction parameter values appropriate to the upper mixed layer of the high latitude oceans. The dynamics of this four-variable system are analysed in terms of the dynamics of much simpler two-variable predator-prey subsystems. Thus, the food web's robust, periodic, four-dimensional dynamics are explained by means of two-dimensional spirals and limit cycles. These dynamical subsystems are coupled by means of an omnivore that transfers control of the dynamics between the two predator-prey subsystems. The food web may substantially decouple the predator-prey subsystems so that the oscillating phytoplankton/zooplankton blooms exhibit population collapses when bacterial 'breathers' briefly dominate after growing dramatically from low background levels. This regular bloom/breather behaviour becomes benignly chaotic when the system is mildly forced by the annual cycle of the sun's irradiance.

1   Key words: Plankton modelling

2   Population dynamics

3   Kolmogorov systems

4

5

1

1. INTRODUCTION

3

Marine plankton ecosystems are being increasingly recognised as a potentially important influence on global climate (Le Quere et al. 2005). Marine plankton ecosystems are an integral component of biogeochemical cycling in the oceans and may have important climate effects due to their ability to draw down carbon dioxide from the atmosphere and store it in the deep ocean (Falkowski et al. 2000) and for their potential to affect cloud formation by producing gases that are eventually transferred to the atmosphere (Charlson et al. 1987). The evaluation of the potential of both of these climatically important processes to affect climate depends critically on understanding the interactions between members of ocean plankton ecosystems, that is, the dynamics of the ecosystem.

13

Generally, the veracity of plankton ecosystem models is evaluated by numerically integrating the models and determining how well they can reproduce observed variables (Le Quere et al. 2005). Typically, ecosystem models are 'calibrated' (the values of parameters describing feeding rates, etc are selected from within a measured range) by comparing model outputs with measured data until the best 'fit' is obtained. The models are then 'validated' by comparing the predictions of the calibrated model with an independent data set. However, a survey of plankton ecosystem models by Arhonditsis and Brett (2004) noted that 95% of plankton ecosystem modelling publications did not report on the model's performance in reproducing all state variables and only 30% quantified the comparison between observed and modelled data. Arhonditsis and Brett observed that about half of modelling papers report that the models were subjected to sensitivity analysis, with a similar proportion validated with independent data.

1 Complex ecosystem models present special problems for this approach, as they often have

2 more parameters than can be constrained by data (Matear 1995).

3

4 The application of plankton ecosystem models in climate modelling has placed additional

5 demands on modellers to develop ever more complex models. (Here we use 'complex' to

6 explicitly mean 'large and complicated', rather than in the context of 'complex systems

7 science' where it is often interpreted to mean irreducible.) Ecosystem models are commonly

8 expressed mathematically as coupled ordinary differential equations (odes) and are often

9 written in a single 'currency', for example in terms of a limiting nutrient such as atomic

10 nitrogen. However, the demands of climate modelling for resolution of the fate of climatically-

11 important gases such as carbon dioxide and dimethyl sulphide in seawater means that these

12 models must also include currencies of carbon and sulphur (Cropp et al. 2004). Similarly, there

13 is increasing evidence that the utilisation of available nitrogen may be limited by the

14 availability of iron, suggesting that iron may also need to be included. If bacterial processes are

15 important, then more than one form of nitrogen may need to be included. The resolution of

16 important processes such as the sinking and export to the deep ocean may require plankton

17 functional types to be included (and consequently even more nutrients explicitly represented),

18 as biogeochemical cycling in marine systems appears closely coupled to particular plankton

19 groups (Anderson 2005). Complex plankton ecosystem models may therefore include 70 state

20 variables (Baretta et al. 1995, Lancelot et al. 2000, Arhonditsis & Brett 2004).

21

22 Mathematical analysis of the dynamics of complex ecosystem models becomes especially

23 difficult when there are three or more state variables and numerical methods must often be

24 employed. Sophisticated numerical integrators are now available that can approximate the

25 dynamics and long-term states of complex ode models; however, vagaries in the

1 implementation of numerical solvers can lead to different results for the same model

2 implementation (Seppelt & Richter 2005), emphasising the importance of more qualitative

3 assessments of ecosystem models. Sensitivity and uncertainty analysis can provide some

4 increased level of confidence in model results by evaluating the sensitivity of the results to

5 variations in the input parameter values. However, sensitivity analysis techniques require many

6 model evaluations, and the computational expense of a global sensitivity analysis of a complex

7 ecosystem model can be prohibitive.

8

9 There is a rich literature attesting to the sensitivity of the dynamics of ode models of

10 ecosystems to small variations in parameter values when, for example, steady states may

11 become oscillatory (Edwards & Brindley 1999). This sensitivity to small parameter variations

12 is especially important for ecosystem models that are coupled to global climate models (Earth

13 System Models) to incorporate ocean biogeochemistry into global climate predictions. The

14 warming of the oceans associated with climate change can affect the parameters of plankton

15 ecosystems in many ways. When simulating ecosystem responses to climate change then, the

16 fact that the models can reproduce current states is no guarantee that the models will correctly

17 predict future climates – the susceptibility of the dynamics of model ecosystems to parameter

18 variations is well-known, and minor parameter changes can lead to significant changes in

19 dynamical behaviours (Kuznetsov & Rinaldi 1996).

20

21 An analytic explication of the factors driving the ecosystem model dynamics can therefore

22 provide a valuable adjunct to numerical techniques. However, nonlinear dynamical systems

23 theory is mostly established for ode models with only two state variables; few theorems extend

24 to three or more variables. An early but often overlooked example of the application of

25 nonlinear dynamical systems theory to ecosystem models is the work of Kolmogorov (1936) in

1 which he developed conditions that ensure that a particular class of two-dimensional predator-

2 prey models, that have come to be called "Kolmogorov systems", have either a stable

3 equilibrium or a stable limit cycle. May (1973) discussed the ecological interpretation of

4 Kolmogorov's theorem, that oscillations in ecosystems either constantly repeat periodically or

5 die out to a stable equilibrium, and noted that it applied to many ecological models then in use.

6 Kolmogorov systems have attracted substantial mathematical interest as they include many

7 types of predator-prey models (Huang & Zhu 2005), but they have been largely ignored by

8 ecologists (Holling 1973).

9 An important issue in ecology is to understand the dynamics of complex trophic systems as a

10 result of the direct interactions between pairs of species. Predator-prey interactions (or, more

11 generally, the interactions between consumers and their resources) are the defining modules in

12 aquatic food webs but it is an open question whether analyses of small subsets of species can

13 provide insights that are relevant to larger communities and ecosystems. In this paper, we

14 explore the insights into the factors controlling the dynamics of complex ecosystems that may

15 be gained by breaking a complex ecosystem model down into its constituent smaller food-web

16 models. Neutel et al. (2002, 2007) used an analogous approach to categorise the properties of

17 real soil micro-organism food-webs, but their subsystems were not self-sustaining. In contrast,

18 we consider only subsystems that are self-sustaining, that is each subsystem we consider could

19 survive as an autonomous unit in the absence of the other organisms in the full food web.

20

21 We examine a moderate complexity marine plankton ecosystem model based on one developed

22 by Moloney et al. (1986) that we have calibrated with parameter values demonstrated to be

23 valid for simulating plankton dynamics in the Barents Sea (Gabric et al. 1999). This model is

24 based on commonly used functional relationships between bacteria (B), zooflagellates (F),

1   phytoplankton (*P*) and zooplankton (*Z*), and includes a limiting nutrient (*N*). The key features

2   of this model are that it is a 'Kolmogorov system' and that it conserves mass.

3

4   Many contemporary ecosystem models (Spitz et al. 2001, Franks 2002, Vallina et al. 2008)

5   may be classed as Kolmogorov systems, as they are of the general form:

6
$$\dot{u}_i = f_i\left(u_1, u_2, \mathsf{K}, u_n\right)u_i, \quad i = 1, 2, \mathsf{K}, n,$$
(1)

7   where $\dot{u} \equiv \dfrac{du}{dt}$ for $t > 0$, and the functions f_i are bounded and continuously differentiable in

8   their variables $u_1, u_2, \mathsf{K}, u_n$. We make the distinction here between a Kolomogorov *system*,

9   which is any system that may be written in the form of (1), and Kolmogorov *conditions*, which

10   describe the conditions on a Kolmogorov system that ensure ecologically realistic dynamics

11   (Kolmogorov 1936). We observe, as did May (1973), that Kolmogorov's conditions may be

12   relaxed whilst still ensuring reasonable dynamics.

13

14   The f_i in equation (1) describe the net growth and mortality of each species, functional type,

15   guild or trophic level, that is $f_i = \left(growth - predation - mortality\right)_i$, and are often nonlinear

16   functions of $u_1, u_2, \mathsf{K}, u_n$. There are many options for the f_i but in accordance with

17   Kolmogorov's (1936) criteria for ecologically realistic dynamics, we choose simple

18   ecologically realistic functions such that the autotrophs are the only variables that can grow at

19   low population concentrations (i.e. $f_a\left(0,0\right) > 0$ and $f_p\left(0,0\right) < 0$) where *a* denotes autotrophs

20   and *p* denotes predators and all other non-autotrophs. Further, increasing population density

21   while maintaining constant ratios of the predators and prey has different effects for predators

22   and prey. The prey is less able to thrive while the predator is more able to thrive as populations

23   increase. In mathematical parlance this is described as $u \cdot \nabla f_a < 0 < u \cdot \nabla f_p$ (May 1973).

1   Ecological realism may also be seen with relation to the $f_a = 0$ and $f_p = 0$ isoclines (for

2   example, Figure 1). Here, we want the f_p isocline to intersect the f_a isocline only once, and to

3   intersect in the manner of the diagram, where for positive α, β, γ we have that $f_a(\alpha, 0) = 0$,

4     $f_a(0, \beta) = 0$ and $f_p(\gamma, 0) = 0$ imply $\alpha > \gamma$ as per Rescigno and Richardson (1967) and May

5   (1973). Note the different scales of intersections in the first two diagrams of the upper panel

6   compared to that of the third: this reflects the different scale of the *B* processes.

7

8   Conservation of mass, or 'closure', depends on there being a currency in terms of which we

9   can measure the concentrations of both the predator and the prey. Here we call this nutrient,

10   and closure means that the total amount of nutrient in the system (the sum of both inorganic

11   and organic forms) remains constant for all time in spite of the complicated interactions

12   between biota. Such conservation of mass is explicit in many models of plankton dynamics

13   (Franks 2002, Gibson et al. 2005), and we also observe that some models that do not explicitly

14   conserve mass fit observed data best when the nutrient uptake and loss fluxes approximately

15   balance (Spitz et al. 2001). Conservation of mass within the mixed layer is also a commonly

16   observed property of marine planktonic ecosystems, that typically cycle nutrient very tightly

17   within the mixed layer of the ocean, and is referred to as regenerated production (Dugdale &

18   Goering 1967). Pragmatically, enforcing conservation of mass in an ecosystem model that is

19   not a Kolmogorov system can in many cases allow it to be written as a Kolmogorov system,

20   allowing the extension of this approach to many other models for the special case where

21   nutrient inputs equal nutrient losses.

22

23   Mathematically, conservation of mass means that, when the scaled variables $u_1, u_2, \mathrm{K}, u_n$ are

24   expressed in terms of the nutrient (*N*) that the variables either feed on or decay into, the total

1   amount of nutrient is conserved and does not change with time; that is

2    $u_1 + u_2 + K + u_n + N = N_T$. This provides a further equation to our Kolmogorov system;

3   although this final equation is not in Kolmogorov form, it is technically redundant as it may be

4   derived directly from the closure of mass condition:

5    $$N = N_T - u_1 - u_2 - K - u_n \quad \Leftrightarrow \quad \dot{N} = -\dot{u}_1 - \dot{u}_2 - K - \dot{u}_n .$$ (2)

6   For a suitably scaled model where the total mass is one unit, the amount of inorganic nutrient

7   (N) present at any time is given by $N = 1 - u_1 - u_2 - K - u_n$; when $\dot{N} > 0$ on $N = 0$ for $u_p > 0$

8   this condition defines an ecologically feasible 'state space' where $0 \leq u_1, u_2, K, u_n \leq 1$ and

9    $u_1 + u_2 + K + u_n \leq 1 \Leftrightarrow N \geq 0$. The dynamics of the system are then confined to the part of a

10   multi-dimensional Cartesian co-ordinate space where each axis represents the (suitably scaled)

11   concentration of the predator or prey and all the variables are positive and less than one. The

12   condition $\sum_{i=1}^{n} u_i \leq 1$ provides a tighter 'lid' on the dynamics. As described by May (1973), such

13   Kolmogorov systems are realistic descriptions of basic ecological models in that populations

14   oscillate for ever or their oscillations gradually decay to come to a stable equilibrium.

15

16   We shall consider a complex food-web system that involves the interconnection of two

17   archetypal predator-prey subsystems, each of which is a Kolmogorov system. The predator-

18   prey subsystems are linked by the omnivorous properties of one of the autotrophs. We observe

19   that our moderate-complexity food web has a very robust stable limit cycle with successive

20   blooms of the biota. The limit cycle is comprised of decaying oscillations ('blooms') of one

21   predator-prey interaction interspersed with occasional outbreaks, that we call 'breathers', of

22   bacteria that are rapidly controlled by their predator. The most interesting aspect of our model,

23   however, is that it demonstrates that the dynamical behaviours of certain realistic complex

1   models can be inferred from the dynamical behaviours of the predator-prey subsystems that

2   comprise them.

3

4   **2. THE PLANKTON MODEL**

5

6   We consider, as an explicit example, a model based on the plankton ecosystem model

7   developed by Moloney et al. (1986). This four-dimensional closed Kolmogorov system was

8   developed from consideration of the allometry of plankton, and has been applied in studies to

9   simulate the response of marine ecosystems to climate change and to model their potential to

10   mitigate the extent of global warming (Gabric et al. 2003). The version of the model we

11   consider has four trophic groups; bacteria (B), zooflagellates (F), phytoplankton (P) and

12   zooplankton (Z) and is written in a currency of the limiting nutrient nitrogen (N). The model,

13   which we shall refer to as the *BFNPZ* model, is comprised of four equations that define the

14   concentration of nutrient contained in each of the biota at any time. The populations of the

15   biota are therefore described in terms of the atomic nitrogen that they contain, rather than

16   numbers of individuals or biomass.

17

18   Each of the model equations is composed of terms that represent each organisms' growth, from

19   consuming inorganic nutrient or other organisms; losses to grazing by their predators; and

20   mortality, including both senescence and losses to predation by higher predators that are only

21   implicitly represented in the model (i.e. are not represented by an equation explicitly describing

22   how their population varies over time). These processes are represented in the model using

23   functional forms commonly utilised in ecosystem models: Michalis-Menten (also called

24   Holling type II) terms for substrate-limited processes such as nutrient uptake or grazing, Lotka-

25   Volterra terms for some grazing functions, and linear mortality terms. The isoclines of these

1 functions are shown in Figure 1. We note that there exists a rich literature describing the

2 dependence of ecosystem model dynamics upon the forms of these terms. However, our

3 predator-prey subsystems contribute all the ecologically-realistic dynamics possible in

4 predator-prey systems, that is both stable spiral equilibrium points and stable limit cycles. We

5 could use other formulations to build our predator-prey subsystems, but this would not

6 contribute predator-prey subsystems with qualitatively different dynamics. Therefore, our

7 specific example reveals some quite general properties

8

9 The four equations of the *BFNPZ* model are:

10
$$\frac{dB}{dt} = f_B B = \left[\frac{k_1(1-k_{11})P}{P+k_2} + \frac{k_{25}(1-k_{11})N}{N+k_{26}} - \frac{k_8 F}{B+k_9} - k_{10} \right] B, \tag{3}$$

11
$$\frac{dF}{dt} = f_F F = \left[\frac{k_8(1-k_{14})B}{B+k_9} - k_{13} \right] F, \tag{4}$$

12
$$\frac{dP}{dt} = f_P P = \left[\frac{k_{23}N}{N+k_{24}} - \frac{k_1 B}{P+k_2} - k_4 Z \right] P, \tag{5}$$

13
$$\frac{dZ}{dt} = f_Z Z = \left[k_4(1-k_{20})P - k_{19} \right] Z. \tag{6}$$

14 The closure of mass condition provides an extra model equation describing the concentration

15 of inorganic nutrient:

16
$$\frac{dN}{dt} = k_{10}B + k_{11}\left[k_{25}\left(\frac{N}{N+k_{26}} \right)B + k_1\left(\frac{P}{P+k_2} \right)B \right] + k_{13}F + k_8 k_{14}\left(\frac{B}{B+k_9} \right)F$$
$$+ k_{19}Z + k_4 k_{20}PZ - k_{23}\left(\frac{N}{N+k_{24}} \right)P - k_{25}\left(\frac{N}{N+k_{26}} \right)B \tag{7}$$

1   As noted above, this equation (7) is not Kolmogorov form but is technically redundant as it

2   may be derived directly from the closure of mass condition:

3    $$N = N_T - B - F - P - Z \quad \Leftrightarrow \quad \frac{dN}{dt} = -\frac{dB}{dt} - \frac{dF}{dt} - \frac{dP}{dt} - \frac{dZ}{dt},$$ (8)

4   where N_T is the total amount of nutrient contained in the system. Note that we could eliminate

5   N from equations (3) - (6) by replacing it with $N_T - B - F - P - Z$, however, we will retain N

6   in the notation for simplicity. Then equations (3)-(6) are four equations in the four variables

7   *BFPZ* of Kolmogorov form, with $0 < B + F + P + Z < 1$ when $0 < B, F, P, Z < 1$ for all time.

8

9   Equations (3) - (6) contain 16 parameters, values for which are based on field measurements

10   that have been validated by simulating plankton dynamics in the Barents Sea (Gabric et al.

11   1999). The model is non-dimensionalised for our analysis; we used the maximum

12   phytoplankton growth rate k_{23} to define a characteristic time scale and define a total nutrient

13   $N_T = 50$ to convert concentrations to proportions of the total. The measured parameter values

14   are then replaced by their scaled equivalents:

15   $$k_m' = \frac{k_m}{k_{23}} \quad \text{for} \quad m = 1, 8, 10, 13, 19, 23 \text{ and } 25,$$ (9)

16   $$k_m' = \frac{k_m}{N_T} \quad \text{for} \quad m = 2, 9, 24 \text{ and } 26,$$ (10)

17   $$k_4' = \frac{k_4 N_T}{k_{23}},$$ (11)

18   $$k_m' = k_m \quad \text{for} \quad m = 11, 14 \text{ and } 20.$$ (12)

1   The measured parameter values and their non-dimensional equivalents are given in Table 1.

2   The general constraints on valid parameter values for the model are that $k_m > 0 \quad \forall \; m$ with the

3   slightly more restrictive constraint for the assimilation efficiency parameters that $0 < k_m < 1$

4   for $m = 11, 14$ and 20. The model is therefore a Kolmogorov *system*, in that it may be written

5   in the form $\dot{u}_i = f_i \left(u_1, u_2, \mathsf{K}, u_n \right) u_i, \quad i = 1, 2, \mathsf{K}, n$, and also meets Kolmogorov's *criteria* for

6   ecologically realistic dynamics of the *BFN* and *NPZ* predator-prey subsystems when

7   parameterised as above.

8

9   **3. REDUCTION TO SUBSYSTEMS**

10

11   The food web described by equations (3) - (6) is depicted in Figure 2 (top centre) with the

12   autonomous food (sub-) webs that comprise it (Figure 2 centre and bottom rows). These

13   subsystems may be obtained from the *BFNPZ* model by setting various state variables

14   identically to zero in equations (3) - (6). The *BFNPZ* system, in that it is composed of the

15   merged *BFNP* and *BNPZ* subsystems. The *BFNP* subsystem is in turn comprised of *BFN* and

16   *BNP* subsystems, while the *BNPZ* subsystem is in turn comprised of *BPN* and *NPZ*

17   subsystems. Diagrams of the trivial autotroph-nutrient systems *BN* and *NP* are not shown

18   separately but are included in the two-variable subsystems. We similarly do not discuss the

19   degenerate food webs (the *BNZ, FNP* and *FNZ* subsystems) that are technically possible but

20   cannot survive in nature, and begin our considerations at the level of the three 'active'

21   subsystems *BFN, BNP* and *NPZ*. We note that the autotrophs *B* and *P* are the 'drivers' of the

22   ecosystem dynamics while the predators *F* and *Z* are 'passive' in that their oscillations and

23   general dynamical behaviour follow that of their prey. Our claim will be that understanding the

24   critical points, and their eigenvalues and eigenvectors, of these subsystems gives us significant

1 insight into the behaviour of the full system. In contrast, we require only of the fully interior

2 point of the full system that it be unstable (which it is for measured parameter values).

3

4 We present vector fields and long-term system trajectories for the *BFNPZ* model and

5 subsystems in Figure 3. This figure demonstrates two important properties of the model:

6 • that the dynamics of the models are mostly confined to near the boundaries

7 (vertices, edges and faces) of the state spaces, and

8 • and that the dynamics of each model can be inferred from the dynamics of its

9 subsystems.

10 We reiterate that the *BFN* and *NPZ* models display the full spectrum of behaviours defined by

11 Kolmogorov (1936) as possible for realistic predator-prey models: a stable limit cycle (*BFN*)

12 and a stable spiral (*NPZ*). While we might explore different process representations in the

13 models and generate different dynamics, the *BFNPZ* model contains all the dynamics that can

14 realistically exist in ecosystem models under Kolmogorov's criteria. Although the vector fields

15 in Figure 3 are specific to the *BFNPZ* model and its sub-models, and to the parameter values

16 used in these models, the dynamics exhibited are general in that the orientation of the arrows of

17 the vector fields in the regions of the spiral critical points is related to, and follows from, the

18 Kolmogorov conditions that encapsulate much intuitive ecological thinking on appropriate

19 predator-prey interaction behaviour. We would therefore expect similar behaviours to be

20 exhibited by the models under parameter variations that maintained the validity of the

21 Kolmogorov conditions, and the interaction omnivore behaviour, and kept the geometry of the

22 fields similar to that shown. Note that the dynamics associated with the unstable predator-prey

23 saddle point and the two stable autotroph nodes of the coupling (*BNP*) model, whilst a

24 Kolmogorov system, do not comply with Kolmogorov's functional form criteria and hence do

25 not exhibit predator-prey dynamics.

1

2

4. CRITICAL POINTS

4

We now examine the critical points of the *BFNPZ* model and note that these are also critical

points of the appropriate subsystems. We will therefore refer to each critical point in bold

italics according to the system for which it is an 'internal' point, for example the critical point

that has $B, F, N \neq 0$ and $P, Z = 0$ will be denoted as the ***BFN*** critical point because it is

internal in that system, but a boundary point in the *BFNP* and *BFNPZ* systems to which it also

belongs. Note that because this nomenclature includes *N* for convenience, each critical point

technically lies in a dimension one less than its name (i.e. the ***N*** point is a point of a zero

dimension system at the origin of the Kolmogorov system, the ***BFN*** point is an interior point

of a two-dimensional system, etc). Similarly, we report only the eigenvalues appropriate for the

number of Kolmogorov dimensions for each point (i.e. the ***BFN*** point will have two

eigenvalues in the *BFN* subsystem, but four in the full *BFNPZ* system).

16

We observe the heuristic that the $f_i = 0$ of each 'feasible' subsystem (that is, not subsystems

such as the *BNZ, FNZ, FNP, BFNZ* or *FNPZ* systems that cannot survive in nature) contribute

a unique expression that identifies an interior point. This expression may have one or several

roots, implying that the point may have simultaneously multiple locations in the state space.

Often only one of these possibilities lies within the ecologically feasible region of the state

space while the others lie outside. This is the case for all the critical points in our model system

with the exception of the ***BNPZ*** point, which for the parameter set used, has only one root and

this root lies outside the ecologically feasible state space. This point is described in the

appendix but is not considered in the analysis as it does not influence the dynamics.

1

2   Analytic expressions for the critical points and their associated eigenvalues (where available)

3   are listed in the appendix with their numerical values calculated from the analytic expressions

4   for the parameter set in Table 1, or derived numerically if analytic expressions for the

5   eigenvalues are not available. The analytic expressions for the critical points and their

6   eigenvalues (where available) reveal the dependency on key parameters. A summary of the

7   critical point locations and their eigenvalues is given in Table 2.

8

9   Table 2 reveals several striking features attesting to the consistency of the system with its

10 subsystems:

11   (i)   the critical points are consistent in each system, in that each system contains an

12   internal critical point plus all the critical points of its subsystems

13   (ii) the eigenvalues (and hence the eigenvectors) of each critical point are the same in

14   each system, that is knowledge of an eigenvalue of a point in a simple system

15   allows that eigenvalue to be inferred for that point of the full system

16   (iii) the addition of extra species (dimensions) to a subsystem adds an eigenvalue to

17   existing critical points that may be inferred from a simpler system, and adds a

18   further internal critical point that may be similar to a subsystem critical point, but

19   for which no information can be inferred a priori from the simpler systems

20   (iv) the eigenvalues of nearby critical points are similar, that is, the vector fields near

21   the critical points are smooth.

22 We observe that features (iii) and (iv) together result in the complex eigenvalues of the *BFN*

23 and *NPZ* predator-prey systems dominating as extra biota are added to form the higher

24 dimension systems.

25

1

5. DYNAMICS

3

4   The consistencies of the critical points of the *BFNPZ* system and its subsystems leads to

5   consistencies in the dynamical behaviours of the *BFNPZ* system and its subsystems (Figure 3).

6   The *BFN* subsystem in Figure 3 (bottom left) exhibits a stable limit cycle, one of the two

7   behaviours permitted under Kolmogorov's conditions. This subsystem includes the **N** saddle

8   point at the origin, the **BN** autotroph point (a saddle in this subsystem) and the unstable spiral

9   **BFN** predator-prey point (labelling as per Table 2). Note that the **N** and **BFN** critical points are

10 located very near each other in the state space. In this case the unstable predator-prey critical

11 point near the origin forces the orbits onto the stable limit cycle, the shape of which is

12 determined by the eigenvectors of the other two critical points on the boundaries. The resultant

13 dynamics are the coexisting populations cycling forever.

14

15 The *NPZ* subsystem (Figure 3, bottom right) demonstrates a (spirally) stable critical point, the

16 alternative behaviour permitted under Kolmogorov's conditions. Again this subsystem includes

17 the **N** saddle point at the origin, the **NP** autotroph point (a saddle in this subsystem), and the

18 stable spiral **NPZ** predator-prey point. This stable spiral point dominates the dynamics in the

19 internal space of this subsystem, while the critical points on the boundaries direct the dynamics

20 into the spiral. This behaviour is that of two species approaching an equilibrium (somewhat

21 slowly in this case) by repeated, but decaying, oscillations.

22

23 The *BNP* subsystem (Figure 3 bottom centre) is not consistent with the Kolmogorov criteria (it

24 remains however a Kolmogorov system) as the co-existence internal predator-prey point is not

25 stable and the system must end up at one of the two stable autotroph points. This interesting

1   dynamic situation is due to *B* acting in this subsystem as an omnivore, that is, simultaneously

2   both an autotroph feeding on *N* and a predator feeding on *P*. This system includes the **N** saddle

3   point at the origin, the **BN** autotroph point, the **NP** autotroph point and a **BNP** predator-prey

4   point. In this subsystem, the **NP** and **BNP** critical points are nearby. The interior **BNP**

5   predator-prey point is a saddle and the two autotroph points (**BN** and **NP**) are both

6   asymptotically stable. The dynamics of the system are therefore that either *B* or *P* dominates

7   the system. The separating surface that determines whether *B* or *P* dominates the subsystem

8   will be discussed below.

9

10 The dynamics of the *BFNP* subsystem (Figure 3 centre left) may be inferred by combining the

11 dynamics of the *BFN* and *BNP* subsystems. This subsystem contains all the critical points (and

12 eigenvalues) of the *BFN* and *BNP* subsystems (**N, BN, NP, BFN** and **BNP**) plus the further

13 **BFNP** unstable spiral internal point. The critical points in this subsystem form groups, with the

14 **N** and **BFN** points paired, and the **NP**, **BNP** and **BFNP** points forming a triple. The dynamics

15 of the *BFNP* subsystem include the stable limit cycle dynamics of the *BFN* subsystem, but

16 these successive *B, F* blooms are quickly overwhelmed by a *P* bloom that initiates when the

17 system passes near the origin (the **N** saddle point) after which the subsystem is attracted along

18 the axis to, and remains at, the stable **NP** autotroph point. Clearly, the separating surface near

19 the origin that determines whether *B* or *P* blooms is critical to these dynamics.

20

21 Consideration of the dynamics of the *NPZ* and *BNP* subsystems similarly provides insight into

22 the dynamics of the *BNPZ* subsystem (Figure 3 centre right). This subsystem contains all the

23 critical points of the *NPZ* and *BNP* subsystems (**N, BN, NP, NPZ** and **BNP**) plus the further

24 **BNPZ** saddle internal point (actually outside the state space in this example). Again the **N** and

25 **BFN** points are paired, as are the **NP** and **BNP** points. In this case, the stable spiral of the *NPZ*

1 subsystem is rendered unstable by the presence of *B* and instead of remaining at this point, the

2 system is initially attracted to it but is eventually directed away from it to the stable **BN**

3 autotroph point. In contrast to the *BFNP* subsystem, the dynamics in this subsystem occur

4 along the unstable eigenvector of the **NPZ** predator-prey point associated with *B*.

5

6 Finally, the dynamics of all the subsystems are evident in the full *BFNPZ* system (Figure 3

7 top). This system includes all the critical points of all the subsystems, although none of these

8 critical points are now stable. In particular, the autotroph critical points **BN** and **NP** that

9 formed the endpoints for the dynamics of the *BFNP* and *BNPZ* subsystems are now both

10 unstable because they both now have grazers feeding on them. Mathematically, the f_i

11 associated with these grazers are positive at these points, and each contributes an unstable

12 eigenvector to the system. Therefore, rather than the dynamics starting with *BFN* dynamics and

13 ending at **NP** as in the *BFNP* subsystem, or starting in *NPZ* dynamics and finishing at **BN** as in

14 the *BNPZ* subsystem, the *BFNPZ* alternates between *BFN* and *NPZ* dynamics in a very robust

15 and stable limit cycle. The shape of this limit cycle is tightly controlled by the eigenvectors and

16 separating surfaces of the subsystems, as will be discussed below.

17

18 We also note that if we consider instead the reduction of the *BFNPZ* system to its subsystems,

19 we are confronted with somewhat counter-intuitive impacts of removing some species. For

20 example, if we remove *F* from the *BFNPZ* system to give the *BNPZ* system we effectively

21 initiate the extinction of the *P* and *Z* populations, as the **BN** critical point is now stable.

22 Similarly, if we remove *Z* from the *BFNPZ* system to give the *BFNP* system we effectively

23 initiate the extinction of the *B* and *F* populations, as the **NP** critical point is now stable.

24

6. THE SIGNPOSTS

The eigenvectors of the critical points on the boundaries of the state space of the *BFNPZ* system, that is the critical points of the subsystems, provide 'signposts' that control the shape of the limit cycle of the system. There are four such signposts; the **N, BN, NP** and **NPZ** critical points. We observe that two of these critical points (**N** and **NP**) are located at vertices of the state space, one (**BN**) is located on an edge and one (**NPZ**) is located on a face, clearly explicating the role that the subsystems play in determining the full system dynamics. These roles are revealed by the vector fields of the *BFNPZ* system in the vicinities of these points (Figures 4 – 7); this will be further discussed below.

We also note that the one fully internal point of the system (the **BFNPZ** point) is important to the dynamics in a different context, in that it (somewhat weakly) repels the system from the interior of the state space so that the vector fields on the boundaries determine the dynamics. Further, the **BFN** critical point associated with the *BFN* subsystem also plays a subtle role on a face of the state space by similarly repelling trajectories and forcing the system to pass very close to the *N* critical point.

The vector field at the origin of the state space (Figure 4) shows that trajectories will be attracted to the origin (the **N** critical point) and then repelled out along the unstable eigenvectors that lie along the *B* and *P* axes. (Note that the eigenvectors lie along the axes of the Kolmogorov state space but are shown in the non-Kolmogorov *BNP* state space.) The eigenvector along the *P* axis has an eigenvalue about 5 times that of the eigenvector along the *B* axis, indicating that *P* will grow faster than *B* in the region of the origin. Note also that the

BFN critical point has a repelling eigenvector, arising from the P competition, pointing into the state space pushing trajectories towards the eigenvector along the P axis.

The vector field along the P axis from the origin maintains trajectories along the axis until this eigenvector joins the corresponding attracting eigenvector, also lying along the P axis, at the **NP** critical point (Figure 5). This is the largest eigenvalue of the 32 eigenvalues of the entire system and is over double the magnitude of the next largest. This is therefore a very influential point in determining the dynamics of the system. The stable eigenvectors of this point all lie along axes of the Kolmogorov state space (the B, F and P axes). The unstable eigenvector points inwards onto the PZ plane towards the **NPZ** critical point.

The imaginary eigenvectors of the spiral **NPZ** critical point (Figure 6) attract the trajectory from the **NP** critical point while the repelling eigenvectors of the **BFNPZ** critical point and the attracting real eigenvector of the **NPZ** critical point force the trajectory onto the PZ plane. The trajectory only leaves this plane when it is pushed out along the unstable real eigenvector of the **NPZ** critical point. This eigenvector arises from the B predation on P, and directs the system through the interior of the state space towards the **BN** critical point. This is the only time the limit cycle of $BFNPZ$ system passes through the interior of the Kolmogorov state space.

The trajectory of the system is rapidly attracted across the state space by the large negative eigenvalues of the **BN** critical point and then directed across the BF plane to the F axis by the large positive eigenvector pointing in that direction. This eigenvector does not point to a critical point, but the trajectories of the system are 'gathered' by the F axis and the vector field indicates they are then directed along the F axis back to the origin where the cycle starts again.

1 The importance and subtlety of the origin in determining the dynamics of the full system, in

2 particular whether B or P blooms is revealed in the next section.

3

4

5 **7. SEPARATING SURFACE AT N CRITICAL POINT**

6

7 The vector field of the BNP subsystem (Figure 8, main panel) reveals the general nature of this

8 'coupling' subsystem that links the BFN and NPZ subsystems. The sample trajectories shown

9 by the solid lines in Figure 8 reveal the influence of the strong negative eigenvalues of the

10 **BNP** critical point in drawing the trajectories to near the boundary of the state space where P

11 dominates the system. The separatrix (dashed line), which separates trajectories that end up at

12 the **BN** critical point from those that end up at the **NP** critical point, suggests that most

13 trajectories of the system will end up at the **BN** critical point. In fact, for almost all cases (in

14 fact for 99% of the state space), B will eventually out-compete P and dominate the long-term

15 state of the system. This figure implies that most initial conditions will result in a B bloom

16 rather than a P bloom. However, the robust limit cycle we observe for the system, in which P

17 consistently blooms at the N critical point, and B consistently blooms only at the **NPZ** critical

18 point suggests that there is more to this story than is revealed by the main panel of Figure 8.

19

20 The region near the origin of Figure 8 is expanded in the inset, which also shows the separating

21 surface (dashed line) that divides the region of the state space where the system will go to the

22 **BN** critical point from the region that will go to the **NP** critical point. We observe that the fates

23 of trajectories that pass near the origin of this state space are very different from those that do

24 not, because the separatrix near the origin asymptotes to the B axis in the vicinity of

25 $B = 0.006$. This reveals that for all concentrations of B lower than this level P will inevitably

dominate the system and bloom. The 'signature' dynamics of the system, with robustly alternating P blooms and B breathers, is therefore critically dependant on the dynamics that occur in the very small region of the state space close to the origin. The separating surface near the N critical point therefore provides a useful insight into the scale of the interactions that are important in understanding the dynamics of this system.

8. BLOOMS AND BREATHERS

We now examine an interesting characteristic that arises from the coupling of the *BFN* system and the *NPZ* system. We will use the term "bloom" to describe the usual dynamics of P rapidly increasing from small levels to dominate the system, and introduce the term "breather" to describe the B outbreaks. This term has been associated with phenomena that emerge from exponentially small states to briefly dominate the system in partial differential equation models. The blooms of B that occur in the *BFNPZ* system for our measured parameter set can be described as breathers as they typically arise from extremely low concentrations. An interesting property of breathers is that they are effectively undetectable at almost all times; in a real ecosystem they would exist at levels that were unmeasurable or of the order of the measurement error. If the breather populations could be detected at times other than during an outbreak, their populations would be observed to be changing very slowly, and an outbreak could not be predicted from sparse knowledge of their changes in population over time.

To emphasise the bloom and breather dynamics, we now essentially decouple the dynamics of the *BFN* subsystem from those of the *NPZ* subsystem by calibrating the *BFNPZ* system with *P* parameter values that are typical of those used to fit *P* dynamics to Southern Ocean satellite

1 chlorophyll dynamics (Gabric et al. 2003). These parameter values result in an *NPZ* system

2 that is highly resilient (i.e. attracts to its *NPZ* spiral point very rapidly) and remains there for a

3 long time before *B* blooms. We then force this system with a sinusoidal cycle that emulates the

4 annual cycle of irradiance in the high latitudes of the Southern Ocean where phytoplankton

5 dynamics are closely related to the annual cycle of irradiance.

6

7 The resulting dynamics of the periodically forced system (Figure 9) reveal the presence of *B*

8 and *F* breathers every $9-13$ years, interrupting the *P* and *Z* blooms that occur annually. The

9 system now exhibits somewhat benign chaos, where the timing and amplitude of the *P, Z*

10 blooms are mostly regular and predictable, but the *B, F* breathers are irregular and effectively

11 unpredictable.

12

13 An important implication for the capacity of systems such as the *BFNPZ* system to generate

14 breathers is a fundamental difference between numerical solvers for ordinary (ode) and partial

15 (pde) differential equations. While robust numerical solvers are available that can accurately

16 solve ode systems and resolve extremely small population sizes, the same cannot be said of

17 numerical solvers for pde systems. The constraints imposed by the requirements of resolving

18 spatial variation in the pde solvers make it difficult to resolve species concentrations to better

19 than one part in a million; whereas breathers typically require a resolution of at least one part in

20 a billion. We therefore observe that the endogenous dynamics that we observe in this analysis,

21 and which are an intrinsic property of the system equations, would not necessarily be observed

22 in models that resolve spatial variation. In particular, the breather dynamics that are evident

23 when populations recover from very low levels would not be reproduced in spatially resolved

24 models by pde solvers.

25

9. DISCUSSION

This research has demonstrated the robust periodic dynamics of a moderate complexity plankton ecosystem model. These dynamics are comprised of regular 'blooms' of phytoplankton and zooplankton followed by 'breathers' of bacteria and zooflagellates that explode from exponentially small levels to briefly dominate the system. We examined the subsystems that comprise this system and noted counterintuitive behaviours. For example, removing the predator (F) of one prey (B) might reasonably be expected to permit the prey population to increase; however, it was not expected that such action would lead to the extinction of a whole related component of the food web (P and Z) leading to the effective collapse of the system. Similarly, removing Z from the system resulted in the dominance of P and the extinction of B and F.

The crucial point of the paper, however, is that we can understand the dynamics of the full system, the blooms and breathers, the robustly repeating cycles of the various individuals' struggle for life, as Rescigno and Richardson (1967) called it, in terms of the key two-variable subsystems. Our results indicate that the behaviour of a complex system can be inferred from the addition of the behaviours of its subsystems.

A key feature of our full dynamical system is that it is Kolmogorov in that each species change in time is proportional to its concentration in the sense that $\dot{u}_i = f_i u_i$. This property is automatically inherited by the subsystems when certain variables $u_j \equiv 0$. However, we note that we require further properties to achieve our realistic dynamics, that is, we need appropriate shapes or functional forms for the various f_i. May (1973) reiterated this point, first made by Kolmogorov (1936), and initiated a tradition of constraining ecosystem models to 'reasonable'

1   functional forms by specifying various derivative conditions, of which we focus on

2    $u_a \nabla f_a < 0 < u_p \nabla f_p$, where a denotes an autotroph and p denotes a predator. Further conditions,

3   which might be specified in terms of isocline intersections (Rescigno & Richardson 1967), are

4   needed so that the key subsystems have only stable spiral attracting points or stable limit

5   cycles, where the populations oscillate eternally. Our *BFN* and *NPZ* systems behave in this

6   manner, and we focus on the mass closure property to help render our full system in this

7   category.

8

9   It is expected that the instability of the interior critical point of the full system means that the

10   dynamics can never rest in its neighbourhood. What is perhaps a little surprising is that other

11   than this, our robust, stable periodic orbit appears not to be directly influenced by the

12   eigenvalues and eigenvectors of this interior point. Instead, our orbit spends most of its time

13   near vertices, edges and faces of the full system state space; i.e. near the **N** critical point (the

14   origin, $N = 1$), the **NP** autotroph point ($P = 1$), the **NPZ** predator-prey point ($P = P^*, Z = Z^*$)

15   and the **BN** autotroph point ($B = B^*$). Physically, this dynamical systems behaviour manifests

16   itself as successive blooms of P and Z interspersed with occasional breathers of B and F. Each

17   population has its turn, even though each regularly decays to levels below 10^{-6} of the total at

18   some point in its life cycle. However, P and Z dominate the system most of the time.

19

20   The addition of an 'annual' forcing, analogous to the effects of seasonal changes in irradiance

21   on phytoplankton, to the system adds a benign chaos to the system. Now, rather than appearing

22   at regular intervals, the breathers become unpredictable, appearing every $9 - 13$ 'years' for our

23   parameter values, chosen to be representative of Southern Ocean values. The precise

24   magnitudes of the various breathers are similarly unpredictable, although the blooms occur

25   with (reasonably) predictable magnitude at regular intervals. The regular bloom and breather

26

behaviour exhibited by the *BFNPZ* system exemplifies the resilience ideas of Holling (1973) where the instability of interior critical points leads to highly resilient systems that are able to robustly persist.

Finally, we note that the endogenous dynamics of the *BFNPZ* system that we have observed by integrating the ordinary differential equations describing the biotic interactions will not necessarily be evident when spatial variation is included and the partial differential equations are solved. This is a result of intrinsic differences between ordinary and partial differential equation solvers. We therefore suggest that when complex ecosystem models are coupled to, for example, ocean circulation models, and when the timing and characteristics of bloom events are critical, then particular care is taken to ensure that the numerical schemes correctly handle small population levels.

10. ACKNOWLEDGEMENTS

1

11. FIGURES AND TABLES

3

Figure Legends

5

Figure 1. Isoclines (upper panels) and function surfaces (lower panels) of the *BFN* (left), *BNP* (middle) and *NPZ* (right) subsystems. The prey isoclines are shown as solid lines and the predator isoclines as dotted lines in the upper panel.

9

Figure 2. Food web of the *BFNPZ* model (top diagram) with the autonomous food webs that may be derived from it: *BFNP* model (middle left); *BNPZ* model (middle right); *BFN* model (bottom left); *BNP* model (bottom centre) and *NPZ* model (bottom right).

13

Figure 3. Vector fields on the faces and dynamics of the *BFNPZ* (top), *BFNP* (middle left), *BNPZ* (middle right), *BFN* (bottom left), *BNP* (bottom centre) and *NPZ* (bottom right) models. We have used *N* as a surrogate for *F* and *Z* in the *BFNPZ* model (top). When the dynamics are in the vicinity of the *BN* (left vertical) plane *N* effectively represents *F*, while when in the vicinity of the *PN* (right vertical) plane *N* effectively represents *Z*. The dynamics on the vertical planes in the top figure are therefore inverted from those of the lower figures.

20

21

Figure 4. Critical points, vector field and eigenvectors in the vicinity of the *N* critical point of the *BFNPZ* system. A part of the *BFNPZ* system limit cycle is also shown.

24

1   Figure 5. Critical points, vector field and eigenvectors in the vicinity of the *P* critical point of

2   the *BFNPZ* system. A part of the *BFNPZ* system limit cycle is also shown.

3

4   Figure 6. Critical points, vector field and eigenvectors in the vicinity of the *NPZ* critical point

5   of the *BFNPZ* system. A part of the *BFNPZ* system limit cycle is also shown.

6

7   Figure 7. Critical points, vector field and eigenvectors in the vicinity of the *BN* critical point of

8   the *BFNPZ* system. A part of the *BFNPZ* system limit cycle is also shown.

9

10   Figure 8. Critical points, vector field and separating surface in the vicinity of the *N*, *P* and *BNP*

11   critical points of the *BFNPZ* system. The dashed line marks the separating surface between

12   initial conditions that go to the *P* critical point (below the dotted line) and those that go to the

13   *BN* critical point (above the dotted line). The solid lines are example trajectories of the system.

14   The region near the origin is blown up in the upper right, lines as for the larger figure.

15

16   Figure 9. Blooms and breathers in the *BFNPZ* system. To create this figure, k_{13} was reduced to

17   0.05 to increase the time between blooms while k_{19} and k_{20} were varied to 0.50 and 0.38

18   respectively to more rapidly dampen the *P* and *Z* oscillations. The *P* maximum growth term

19   was forced with an equivalent annual cycle of irradiance $k_{23}^{"} = k_{23} + 0.5\sin(0.02\pi t)$.

20

21

22   **Tables**

23

24

25   Table 1: Parameter values used for the *BFNPZ* model.

1

PAR	PROCESS	UNITS	RAW	SCALED	REFERENCE
k_1	Max rate of N uptake by B	d^{-1}	0.31	1.148	Muller-Niklas and Herndl (1996)
k_2	Half-sat const for B uptake of N	$mgNm^{-3}$	34.65	0.693	Moloney et al. (1986)
k_4	Z grazing rate (per ind) on P	$m^3mgN^{-1}d^{-1}$	0.01	1.852	Gabric et al. (1999)
k_8	Max rate of B uptake by F	d^{-1}	1.67	6.185	Hansen et al. (1996)
k_9	Half-sat const for F uptake of B	$mgNm^{-3}$	9.10	0.182	Fenchel (1982)
k_{10}	B specific excretion rate	d^{-1}	0.07	0.259	Moloney et al. (1986)
k_{11}	Prop of N uptake excreted by B	-	0.63	0.63	Moloney et al. (1986)
k_{13}	F specific excretion rate	d^{-1}	0.05	0.1851	Moloney et al. (1986)
k_{14}	Prop of N uptake excreted by F	-	0.65	0.65	Moloney et al. (1986)
k_{19}	Z specific N excretion rate	d^{-1}	0.05	0.1852	Moloney et al. (1986)
k_{20}	Prop of N uptake excreted by Z	-	0.40	0.40	Moloney et al. (1986)
k_{23}	Max rate of N uptake by P	d^{-1}	0.27	1	Gabric et al. (1999)
k_{24}	Half-sat const for P uptake of N	$mgNm^{-3}$	12.60	0.252	Slagstad and Stole-Hansen (1991)
k_{25}	Max rate of N uptake by B	d^{-1}	0.31	1.148	Muller-Niklas and Herndl (1996)
k_{26}	Half-sat const for B uptake of N	$mgNm^{-3}$	3.45	0.069	Billen and Becquevort (1991)
N_T	Total nutrient as nitrogen	$mgNm^{-3}$	50	1	Gabric et al. (1999)

2

3

Table 2. Critical point values and associated eigenvalues.

CP	SYS	B^*	F^*	N^*	P^*	Z^*	λ_1	λ_2	λ_3	λ_4	ST[1]
N	**BN**	0	-	1	-	-	0.1383	-	-	-	US
	NP	-	-	1	0	-	-	-	0.7987	-	US
	BFN	0	0	1			0.1383	-0.1851	-	-	SAD
	BNP	0	-	1	0	-	0.1383	-	0.7987	-	US
	NPZ	-	-	1	0	0	-	-	0.7987	-0.1852	SAD
	BFNP	0	0	1	0	-	0.1383	-0.1851	0.7987	-	SAD
	BNPZ	0	-	1	0	0	0.1383	-	0.7987	-0.1852	SAD
	BFNPZ	0	0	1	0	0	0.1383	-0.1851	0.7987	-0.1852	SAD
BN	**BN**	0.8919	-	0.1081		-	-0.8364	-	-	-	AS
	BFN	0.8919	0	0.1081	-	-	-0.8364	1.6129	-	-	SAD
	BNP	0.8919	-	0.1081	0	-	-0.8364	-	-1.1783	-	AS
	BFNP	0.8919	0	0.1081	0	-	-0.8364	1.6129	-1.1783	-	SAD
	BNPZ	0.8919	-	0.1081	0	0	-0.8364	-	-1.1783	-0.1852	AS
	BFNPZ	0.8919	0	0.1081	0	0	-0.8364	1.6129	-1.1783	-0.1852	SAD
NP	**NP**	-	-	0	1	-	-	-	-3.9683	-	AS
	BNP	0	-	0	1	-	-0.0081	-	-3.9683	-	AS
	NPZ	-	-	0	1	0	-	-	-3.9683	0.9260	SAD
	BFNP	0	0	0	1	0	-0.0081	-0.1851	-3.9683	-	AS
	BNPZ	0	0	0	1	0	-0.0081	-	-3.9683	0.9260	SAD
	BFNPZ	0	0	0	1	0	-0.0081	-0.1851	-3.9683	0.9260	SAD
BFN	**BFN**	0.0170	0.0044	0.9785	-	-	$0.0057 \pm 0.1527i$		-	-	US
	BFNP	0.0170	0.0044	0.9785	0	-	$0.0057 \pm 0.1527i$		0.7670	-	US
	BFNPZ	0.0170	0.0044	0.9785	0	0	$0.0057 \pm 0.1527i$		0.7670	-0.1852	SSAD
BNP	**BNP**	0.0091	-	0.0016	0.9894	-	0.0079	-	-3.9365	-	SAD
	BNPZ	0.0091	-	0.0016	0.9894	0	0.0079	-	-3.9365	0.9145	SAD

	BFNPZ	0.0091	0	0.0016	0.9894	0	0.0079	-0.0852	-3.9365	0.9145	SAD
NPZ	*NPZ*	-	-	0.4794	0.1667	0.3539	-	-	$-0.0393 \pm 0.3882i$		SS
	BNPZ	0	-	0.4794	0.1667	0.3539	0.1947	-	$-0.0393 \pm 0.3882i$		US
	BFNPZ	0	0	0.4794	0.1667	0.3539	0.1947	-0.1851	$-0.0393 \pm 0.3882i$		SSAD
BFNP[2]	*BFNP*	0.0170	0.0002	0.0030	0.9798	-	$0.0076 \pm 0.0340i$		-3.9017	-	SSAD
	BFNPZ	0.0170	0.0002	0.0030	0.9798	0	$0.0076 \pm 0.0340i$		-3.9017	0.9037	SSAD
BFNPZ[2]	*BFNPZ*	0.0170	0.0062	0.4707	0.1667	0.3394	$0.0079 \pm 0.1799i$		$-0.0384 \pm 0.3839i$		SSAD

[1] SAD denotes a saddle point (unstable in at least one dimension), SSAD denotes a spiral saddle point, AS denotes an asymptotically stable point, SS denotes a spirally stable point and US denotes an unstable node.

[2] Eigenvalues were calculated numerically for the *BFNP* and *BFNPZ* points except for λ_4 of the *BFNP* point for which an analytic expression was obtained (see appendix).

12. LITERATURE CITED

Anderson TR (2005) Plankton functional type modelling: running before we can walk? J Plankton Res 27:1073-1081

Arhonditsis GB, Brett MT (2004) Evaluation of the current state of mechanistic aquatic biogeochemical modeling. . Marine Ecology Progress Series 271:13-26

Baretta J, Ebenhoh W, Ruardij P (1995) The European Regional Seas Ecosystem Model, a complex marine ecosystem model. Journal of Sea Research 33:233-246

Charlson RJ, Lovelock JE, Andreae MO, Warren SG (1987) Oceanic phytoplankton, atmospheric sulphur, cloud albedo and climate. Nature 326:655-661

Cropp RA, Norbury J, Gabric AJ, R. D. Braddock (2004), Global Biogeochem. Cycles, 18, (2004) Modeling dimethylsulphide production in the upper ocean. Global Biogeochemical Cycles 18:doi:10.1029/2003GB002126.

Dugdale RC, Goering JJ (1967) Uptake of new and regenerated forms of nitrogen in primary productivity. Limnology and Oceanography 12:196-206

Edwards AM, Brindley J (1999) Zooplankton mortality and the dynamical behaviour of plankton population models. Bulletin Of Mathematical Biology 61:303-339

Falkowski P, Scholes RJ, Boyle E, Canadell J, Canfield D, Elser J, Gruber N, Hibbard K, Hogberg P, Linder S, Mackenzie FT, Moore B, Pedersen T, Rosenthal Y, Seitzinger S, Smetacek V, Steffen W (2000) The global carbon cycle: A test of our knowledge of the Earth as a system. Science 290:291-296

Franks PJS (2002) NPZ models of plankton dynamics: their construction, coupling to physics, and application. Journal of Oceanography 58:379-387

Gabric AJ, Cropp RA, Hirst AC, Marchant HJ (2003) The response of dimethylsulphide production to simulated warming in the eastern Antarctic Southern Ocean. Tellus 55B:966-981

Gabric AJ, Matrai PA, Vernet M (1999) Modelling the production and cycling of dimethylsulphide during the vernal bloom in the Barents Sea. Tellus 51B:919-937

Gibson G, Musgrave D, Hinckley S (2005) Non-linear dynamics of a pelagic ecosystem model with multiple predator and prey types. Journal of Plankton Research 27:427-447

Holling CS (1973) Resilience and stability of ecological systems. Annual Review of Ecology and Systematics 4:1-23

Huang XC, Zhu L (2005) Limit cycles in a general Kolmogorov model. Nonlinear Analysis 60:1393-1414

Kolmogorov AN (1936) Sulla Teoria di Volterra della Lotta per l'Esisttenza. Giorn Instituto Ital Attuari 7:74-80

Kuznetsov Y, Rinaldi S (1996) Remarks on Food Chain Dynamics. Mathematical Biosciences 134:1-33

Lancelot C, Hannon E, Becquevort S, Veth C, De Baar HJW (2000) Modeling phytoplankton blooms and carbon export production in the Southern Ocean: dominant controls by light and iron in the Atlantic sector in Austral spring 1992. Deep-Sea Research I 47:1621-1662

Le Quere C, Harrison SP, Prentice IC, Buitenhuis ET, Aumonts O, Bopp L, Claustre H, Cotrim da Cunha L, Geider RJ, Giraud X, Klaas C, Kohfeld KE, Legrende L, Manizza M, Platt T, Rivkin RB, Sathyendranath S, Uitz J, Watson A, Wolf-Gladrow D (2005) Ecosystem

dynamics based on plankton functional types for global ocean biogeochemistry models. Global Change Biology 11:2016-2040

Matear RJ (1995) Parameter optimization and analysis of ecosystem models using simulated annealing: A case study at Station P. Journal of Marine Research 53:571-607

May RM (1973) Stability and Complexity in Model Ecosystems., Vol. Princeton University Press, Princeton

Moloney CL, Bergh MO, Field JG, Newell RC (1986) The effect of sedimentation and microbial nitrogen regeneration in a plankton community: a simulation investigation. Journal of Plankton Research 8:427-445

Neutel A-M, Heesterbeek JAP, de Ruiter PC (2002) Stability in real food webs: Weak links in long loops. Science 296:1120-1123

Neutel A-M, Heesterbeek JAP, van de Koppel J, Hoenderboom G, Vos A, Kaldeway C, Berendse F, de Ruiter PC (2007) Reconciling complexity with stability in naturally assembling food webs. Nature 449:599-602

Rescigno A, Richardson IW (1967) The Struggle for Life I. Two Species. Bull Mathematical Biophysics 29:377-388

Seppelt R, Richter O (2005) "It was an artefact not the result": A note on systems dynamic model development tools. Environmental Modelling And Software 20:1543-1548

Spitz YH, Moisan JR, Abbott MR (2001) Configuring an ecosystem model using data from the Bermuda Atlantic Time Series (BATS). Deep-Sea Research II 48:1733-1768

Vallina SM, Simo R, Popova EE, Anderson TR, Gabric A, Cropp RA, Pacheco JM (2008) A dynamic model of ocean sulfur (DMOS) applied to the Sargasso Sea: simulating the dimethylsulfide (DMS) summer paradox. Journal of Geophysical Research (Biogeosciences) 113:G01009, doi:01010.01029/02007JG000415

13. APPENDIX

N critical point

In common with all Kolmogorov models, the *BFNPZ* model has a critical point at the origin of the system where no biota are extant:

$$N_N^* = 1, \tag{13}$$

$$B_N^*, F_N^*, P_N^*, Z_N^* = 0. \tag{14}$$

The eigenvalues of the Jacobian at this point are:

$$\lambda_{N-1} = \frac{k_{25}\left(1 - k_{11}\right)}{1 + k_{26}} - k_{10} = 0.1383, \tag{15}$$

$$\lambda_{N-2} = -k_{13} = -0.1851, \tag{16}$$

$$\lambda_{N-3} = \frac{k_{23}}{1 + k_{24}} = 0.7987, \tag{17}$$

$$\lambda_{N-4} = -k_{19} = -0.1852. \tag{18}$$

The eigenvectors associated with these eigenvalues all point along the species axes, with the unstable autotroph eigenvectors associated with λ_{N-1} and λ_{N-3} pointing along the *B* and *P* axes respectively.

BN critical point

The first autotroph critical point of the *BFNPZ* model is given by:

$$B^*_{BN} = 1 - \frac{k_{10}k_{26}}{k_{25}\left(1 - k_{11}\right) - k_{10}} = 0.8919, \tag{19}$$

$$N^*_{BN} = \frac{k_{10}k_{26}}{k_{25}\left(1 - k_{11}\right) - k_{10}} = 0.1081, \tag{20}$$

$$F^*_{BN}, P^*_{BN}, Z^*_{BN} = 0. \tag{21}$$

The eigenvalues of this point are:

$$\lambda_{BN-1} = k_{25}\left(1 - k_{11}\right)\left(\frac{N^{*}{}^2_{BN} + k_{26}\left(N^*_{BN} - B^*_{BN}\right)}{\left(N^*_{BN} + k_{26}\right)^2}\right) - k_{10} = -0.8364, \tag{22}$$

$$\lambda_{BN-2} = k_8\left(1 - k_{14}\right)\left(\frac{B^*_{BN}}{B^*_{BN} + k_9}\right) - k_{13} = 1.6129, \tag{23}$$

$$\lambda_{BN-3} = k_{23}\left(\frac{N^*_{BN}}{N^*_{BN} + k_{24}}\right) - \left(\frac{k_1}{k_2}\right)B^*_{BN} = -1.1783, \tag{24}$$

$$\lambda_{BN-4} = -k_{19} = -0.1852. \tag{25}$$

The eigenvectors associated with these eigenvalues again all point along the species axes, with the exception of the unstable eigenvector associated with λ_{BN-2} which points internally towards the *F* axis. Note that the λ_{N-1} eigenvector pointing away from the *N* critical point

joins the λ_{BN-1} eigenvector pointing into the **BN** critical point. A *B* bloom initiated at the origin must therefore end up at the **BN** critical point.

NP critical point

The second autotroph-only critical point of the model is:

$$P_{NP}^* = 1, \tag{26}$$

$$B_{NP}^*, F_{NP}^*, N_{NP}^*, Z_{NP}^* = 0. \tag{27}$$

The eigenvalues of this point are:

$$\lambda_{NP-1} = \frac{k_1\left(1-k_{11}\right)}{1+k_2} - k_{10} = -0.0081, \tag{28}$$

$$\lambda_{NP-2} = -k_{13} = -0.1851, \tag{29}$$

$$\lambda_{NP-3} = -\frac{k_{23}}{k_{24}} = -3.9683, \tag{30}$$

$$\lambda_{NP-4} = k_4\left(1-k_{20}\right) - k_{19} = 0.9620. \tag{31}$$

Once again, the eigenvectors associated with these eigenvalues again all point along the species axes, with the exception of the unstable eigenvector associated with λ_{NP-4} which points along a separatrix into the *NPZ* plane. Note in this case that the λ_{N-3} eigenvector pointing away from the *N* critical point joins the λ_{NP-3} eigenvector pointing into the **NP** critical point. A *P* bloom initiated at the origin must therefore end up at the **NP** critical point.

BFN critical point

The first predator-prey critical point of the *BFNPZ* model is at:

$$B^*_{BFN} = \frac{k_9 k_{13}}{k_8\left(1 - k_{14}\right) - k_{13}} = 0.0170, \tag{32}$$

$$F^*_{BFN} = \frac{k_{25}}{k_8}\left(1 - k_{11}\right)\left(B^*_{BFN} + k_9\right)\left(\frac{N^*_{BFN}}{N^*_{BFN} + k_{26}}\right) - \frac{k_{10}}{k_8}\left(B^*_{BFN} + k_9\right) = 0.0044, \tag{33}$$

$$N^*_{BFN} = \frac{1}{2}\left[\begin{array}{c} -\left(k_{26} + B^*_{BFN} + \left(\frac{B^*_{BFN} + k_9}{k_8}\right)\left(k_{25}\left(1 - k_{11}\right) - k_{10}\right) - 1\right) \\ \pm\sqrt{\left(k_{26} + B^*_{BFN} + \left(\frac{B^*_{BFN} + k_9}{k_8}\right)\left(k_{25}\left(1 - k_{11}\right) - k_{10}\right) - 1\right)^2 \\ -4k_{26}\left(B^*_{BFN} - 1 + k_{10}\left(\frac{B^*_{BFN} + k_9}{k_8}\right)\right)} \end{array}\right] = 0.9785, \tag{34}$$

$$P^*_{BFN}, Z^*_{BFN} = 0. \tag{35}$$

The eigenvalues at this point are:

$$\text{Re}\left(\lambda_{BFN-1,2}\right) = k_8\left(\frac{B^*_{BFN}}{\left(B^*_{BFN} + k_9\right)^2}\right) - k_{25}\left(1 - k_{11}\right)\left(\frac{k_{26}}{\left(N^*_{BFN} + k_{26}\right)^2}\right)B^*_{BFN} = 0.0057, \tag{36}$$

$$\text{Im}\left(\lambda_{BFN-1,2}\right) = \pm \left\{ \left[\left[k_8 \left(\frac{B^*_{BFN}}{\left(B^*_{BFN} + k_9\right)^2} \right) F^*_{BFN} - k_{25}\left(1 - k_{11}\right) \left(\frac{k_{26}}{\left(N^*_{BFN} + k_{26}\right)^2} \right) B^*_{BFN} \right]^2 - 4 \left[k_{25}\left(1 - k_{11}\right) \left(\frac{k_{26}}{\left(N^*_{BFN} + k_{26}\right)^2} \right) B^*_{BFN} + k_8 \left(\frac{B^*_{BFN}}{B^*_{BFN} + k_9} \right) \right] \times \left[k_8\left(1 - k_{14}\right) \left(\frac{k_9}{\left(B^*_{BFN} + k_9\right)^2} \right) F^*_{BFN} \right] \right\}^{1/2}$$

$$= \pm 0.1527i, \tag{37}$$

$$\lambda_{BFN-3} = k_{23}\left(\frac{N^*_{BFN}}{N^*_{BFN} + k_{24}} \right) - \left(\frac{k_1}{k_2} \right) B^*_{BFN} = 0.7670, \tag{38}$$

$$\lambda_{BFN-4} = -k_{19} = -0.1852. \tag{39}$$

The unstable eigenvectors of this point push orbits towards the origin, from where the orbit is directed to the **NP** autotroph critical point.

BNP critical point

The second predator-prey critical point (technically an omnivore-prey critical point as *B* consumes both *N* and *P*) is given by:

$$B^*_{BNP} = \frac{k_{23}\left(P^*_{BNP} + k_2\right)N^*_{BNP}}{k_1\left(N^*_{BNP} + k_{24}\right)} = 0.0091, \tag{40}$$

$$\alpha N^{*3}_{BNP} + \beta N^{*2}_{BNP} + \chi N^*_{BNP} + \delta = 0 \quad \Rightarrow N^*_{BNP} = 0.0016, \tag{41}$$

$$P^*_{BNP} = \frac{k_2\left[k_{10}\left(N^*_{BNP} + k_{26}\right) - k_{25}\left(1 - k_{11}\right)N^*_{BNP} \right]}{k_1\left(1 - k_{11}\right)\left(N^*_{BNP} + k_{26}\right) + k_{25}\left(1 - k_{11}\right)N^*_{BNP} - k_{10}\left(N^*_{BNP} + k_{26}\right)} = 0.9894, \tag{42}$$

$$F^*_{BNP}, Z^*_{BNP} = 0 , \tag{43}$$

where: $\alpha = k_1 \left[k_1 + k_{25} - k_{10} - k_{11} \left(k_1 + k_{25} \right) \right],$

$$\beta = k_1 \begin{bmatrix} k_{11} \left(k_{25} \left\{ 1 - k_{24} + k_2 \right\} + k_1 \left\{ 1 - k_{24} - k_{26} \right\} - k_2 k_{23} \right) + k_1 \left(k_{24} + k_{26} - 1 \right) \\ -k_{10} \left(k_{26} - k_2 + k_{24} - 1 \right) + k_2 k_{23} - k_{25} \left(k_2 - k_{24} + 1 \right) \end{bmatrix},$$

$$\chi = k_1 \begin{bmatrix} k_1 \left(k_{26} \left\{ k_{24} - 1 + k_{11} \right\} - k_{24} + k_{11} k_{24} \left\{ 1 - k_{26} \right\} \right) \\ + k_{24} k_{25} \left(1 + k_2 \right)\left(k_{11} - 1 \right) + k_{10} k_{26} \left(1 + k_2 \right) \\ + k_2 k_{23} k_{26} \left(1 - k_{11} \right) + k_{10} k_{24} \left(1 + k_2 - k_{26} \right) \end{bmatrix},$$

$$\delta = k_1 \left[k_{24} k_{26} \left(k_{10} \left\{ k_2 + 1 \right\} - k_1 \left\{ 1 - k_{11} \right\} \right) \right].$$

The eigenvalues at this point are:

$$\lambda_{BNP-1} = \frac{\alpha' + \beta' + \sqrt{\left(\alpha' + \beta' \right)^2 + 4 \chi' \delta'}}{2} = 0.0079 , \tag{44}$$

$$\lambda_{BNP-2} = k_8 \left(1 - k_{14} \right)\left(\frac{B^*_{BNP}}{B^*_{BNP} + k_9} \right) - k_{13} = -0.0852 , \tag{45}$$

$$\lambda_{BNP-3} = \frac{\alpha' + \beta' - \sqrt{\left(\alpha' + \beta' \right)^2 + 4 \chi' \delta'}}{2} = -3.9365 , \tag{46}$$

$$\lambda_{BNP-4} = k_4 \left(1 - k_{20} \right) P^*_{BNP} - k_{19} = 0.9145 , \tag{47}$$

where

$$\alpha' = k_1 \left(1 - k_{11}\right) \left(\frac{P^*_{BNP}}{P^*_{BNP} + k_2} \right) + k_{25} \left(1 - k_{11}\right) \left(\frac{N^*_{BNP}}{N^*_{BNP} + k_{26}} \right)$$

$$- k_{25} \left(1 - k_{11}\right) \left(\frac{k_{26}}{\left(N^*_{BNP} + k_{26}\right)^2} \right) B^*_{BNP} - k_{10}, \tag{48}$$

$$\beta' = k_{23} \left(\frac{N^*_{BNP}}{N^*_{BNP} + k_{24}} \right) - k_{23} \left(\frac{k_{24}}{\left(N^*_{BNP} + k_{24}\right)^2} \right) P^*_{BNP} - k_1 \left(\frac{k_2}{\left(P^*_{BNP} + k_2\right)^2} \right) B^*_{BNP}, \tag{49}$$

$$\chi' = -k_{23} \left(\frac{k_{24}}{\left(N^*_{BNP} + k_{24}\right)^2} \right) P^*_{BNP} - k_1 \left(\frac{P^*_{BNP}}{P^*_{BNP} + k_2} \right), \tag{50}$$

$$\delta' = -k_1 \left(1 - k_{11}\right) \left(\frac{k_2}{\left(P^*_{BNP} + k_2\right)^2} \right) B^*_{BNP}. \tag{51}$$

NPZ critical point

The third predator-prey critical point of the model is given by:

$$B^*_{NPZ}, F^*_{NPZ} = 0, \tag{52}$$

$$N^*_{NPZ} = \frac{1}{2} \left[-\left(k_{24} + P^*_{NPZ} + \frac{k_{23}}{k_4} - 1 \right) \pm \sqrt{ \left(k_{24} + P^*_{NPZ} + \frac{k_{23}}{k_4} - 1 \right)^2 - 4 k_{24} \left(P^*_{NPZ} - 1 \right) } \right], \tag{53}$$

$$= 0.4794$$

$$P^*_{NPZ} = \frac{k_{19}}{k_4 \left(1 - k_{20}\right)} = 0.1667, \tag{54}$$

41

$$Z^*_{NPZ} = \frac{k_{23}}{k_4}\left(\frac{N^*_{NPZ}}{N^*_{NPZ} + k_{24}}\right) = 0.3539.\tag{55}$$

The eigenvalues at this point are:

$$\lambda_{NPZ-1} = k_1\left(1 - k_{11}\right)\left(\frac{P^*_{NPZ}}{P^*_{NPZ} + k_2}\right) + k_{25}\left(1 - k_{11}\right)\left(\frac{N^*_{NPZ}}{N^*_{NPZ} + k_{26}}\right) - k_{10} = 0.1947,\tag{56}$$

$$\lambda_{NPZ-2} = -k_{13} = -0.1851,\tag{57}$$

$$\mathrm{Re}\left(\lambda_{NPZ-3,4}\right) = -\frac{k_{23}P^*_{NPZ}}{2}\left[\frac{k_{24}}{\left(N^*_{NPZ} + k_{24}\right)^2}\right] = -0.0393,\tag{58}$$

$$\mathrm{Im}\left(\lambda_{NPZ-3,4}\right) = \pm\frac{1}{2}\sqrt{\left\{k_{23}P^*_{NPZ}\left[\frac{k_{24}}{\left(N^*_{NPZ} + k_{24}\right)^2}\right]\right\}^2 + 4k_4\left(1 - k_{20}\right)\left\{k_{23}\left[\frac{k_{24}}{\left(N^*_{NPZ} + k_{24}\right)^2}\right] - k_4\right\}P^*_{NPZ}Z^*_{NPZ}} = \pm 0.3882i.\tag{59}$$

The unstable eigenvector associated with λ_{NPZ-1} points toward the **BN** autotroph critical point.

BFNP critical point

The first higher-dimension food web critical point, where four of the five state variables are non-zero, is given by:

$$B^*_{BFNP} = \frac{k_9 k_{13}}{k_8 \left(1 - k_{14}\right) - k_{13}} = 0.0170 \,, \tag{60}$$

$$F^*_{BFNP} = \frac{k_{25}}{k_8} \left(1 - k_{11}\right) \left(B^*_{BFNP} + k_9\right) \left(\frac{N^*_{BFNP}}{N^*_{BFNP} + k_{26}}\right) - \frac{k_{10}}{k_8} \left(B^*_{BFNP} + k_9\right) = 0.0002 \,, \tag{61}$$

$$N^{*\,4}_{BFNP} + N^{*\,3}_{BFNP}\left[k_{26} + k_{24} - 1 - k_2 + B^*_{BFNP} - \beta k_{10} + \alpha + \beta\gamma\left(1 - \frac{k_2}{\alpha}\right) + \beta\delta\right]$$

$$+ N^{*\,2}_{BFNP}\left[\begin{array}{c} k_{26}\left(k_{24} - 1 - k_2 + B^*_{BFNP} - \beta k_{10} + \alpha + \beta\gamma\left(1 - \frac{k_2}{\alpha}\right)\right) + \alpha k_{24} \\ - k_{24}\left(1 + k_2 - B^*_{BFNP} + \beta k_{10} - \alpha\right) + \beta k_{24}\left(\delta + \gamma\right) \end{array}\right] \tag{62}$$

$$+ N^*_{BFNP}\left[\alpha k_{24}^2 + k_{26}\left(\alpha k_{24} - k_{24}\left[1 + k_2 - B^*_{BFNP} + \beta k_{10} - \alpha\right] + \beta\gamma k_{24}\right)\right] + \alpha k_{24}^2 k_{26} = 0$$

$$\Rightarrow N^*_{BFNP} = 0.0030,$$

$$P^*_{BFNP} = \frac{k_1}{k_{23}}\left(\frac{N + k_{24}}{N}\right)B^*_{BFNP} - k_2 = 0.9798 \,, \tag{63}$$

$$Z^*_{BFNP} = 0 \,, \tag{64}$$

where $\alpha = \dfrac{k_1 B^*_{BFNP}}{k_{23}}$, $\beta = \dfrac{B^*_{BFNP} + k_9}{k_8}$, $\delta = k_{25}\left(1 - k_{11}\right)$, $\varepsilon = \dfrac{k_2 k_{23}}{k_1 B^*_{BFNP}}$ and $\gamma = k_1\left(1 - k_{11}\right)$ and only

the positive roots are ecologically feasible.

Analytic expressions for most of the eigenvalues at the *BFNP* point are not useful, and these eigenvalues will be calculated numerically. However, the analytic expression for the eigenvalue associated with the *Z* dimension is informative:

$$\lambda_{BFNP-4} = k_4\left(1 - k_{20}\right)P^*_{BFNP} - k_{19} = 0.9037 \,. \tag{65}$$

We note from comparison with the numerically calculated eigenvalues listed in Table 3 that the λ_{BFNP-4} eigenvalue is the most unstable direction at this critical point, by a factor of about 100.

BNPZ critical point

The second higher-dimension food web critical point, where four of the five state variables are non-zero, is given by:

$$B^*_{BNPZ} = \frac{\left(P^*_{BNPZ} + k_2\right)\left[1 - N^*_{BNPZ} - P^*_{BNPZ} - \frac{k_{23}}{k_4}\left(\frac{N^*_{BNPZ}}{N^*_{BNPZ} + k_{24}}\right)\right]}{P^*_{BNPZ} + k_2 - \frac{k_1}{k_4}} = 2.4959, \quad (66)$$

$$F^*_{BNPZ} = 0, \quad (67)$$

$$N^*_{BNPZ} = \frac{k_{26}\left[k_1\left(1 - k_{11}\right)P^*_{BNPZ} - k_{10}\left(P^*_{BNPZ} + k_2\right)\right]}{\left(P^*_{BNPZ} + k_2\right)\left[k_{10} - k_{25}\left(1 - k_{11}\right)\right] - k_1\left(1 - k_{11}\right)P^*_{BNPZ}} = 0.0492, \quad (68)$$

$$P^*_{BNPZ} = \frac{k_{19}}{k_4\left(1 - k_{20}\right)} = 0.1667, \quad (69)$$

$$Z^*_{BNPZ} = \frac{k_{23}}{k_4}\left(\frac{N^*_{BNPZ}}{N^*_{BNPZ} + k_{24}}\right) - \frac{k_1}{k_4}\left(\frac{B^*_{BNPZ}}{P^*_{BNPZ} + k_2}\right) = -1.7118. \quad (70)$$

Analytic expressions for most of the eigenvalues at the *BNPZ* point are not useful, and these eigenvalues will be calculated numerically. However, the analytic expression for the eigenvalue associated with the *F* dimension is informative:

$$\lambda_{BNPZ-2} = k_8\left(1 - k_{14}\right)\left(\frac{B^*_{BNPZ}}{B^*_{BNPZ} + k_9}\right) - k_{13} = 1.8326. \quad (71)$$

Note that for the parameter values used in the model, this point lies outside the ecologically feasible region of the state space, and the eigenvalues do not have any influence on the dynamics of the system. We further note that this point may be brought into the feasible state space with subtle variations of certain parameter values.

BFNPZ critical point

The final critical point of the *BFNPZ* model, that is not shared by any of the sub-models, the only critical point to have all positive, non-zero state variables (i.e. the only 'interior' point of the full model) is:

$$B^*_{BFNPZ} = \frac{k_9 k_{13}}{k_8 \left(1 - k_{14}\right) - k_{13}} = 0.0170,$$ (72)

$$F^*_{BFNPZ} = \left(\frac{B^*_{BFNPZ} + k_9}{k_8}\right) \left[k_1 \left(1 - k_{11}\right) \left(\frac{P^*_{BFNPZ}}{P^*_{BFNPZ} + k_2}\right) + k_{25} \left(1 - k_{11}\right) \left(\frac{N^*_{BFNPZ}}{N^*_{BFNPZ} + k_{26}}\right) - k_{10} \right]$$ (73)
$$= 0.0062,$$

$$N^{*3}_{BFNPZ} + N^{*2}_{BFNPZ} \left[P^*_{BFNPZ} + B^*_{BFNPZ} + \alpha + \beta + \delta + k_{24} + k_{26} - \gamma - \varepsilon - 1 \right] +$$
$$N^*_{BFNPZ} \left[k_{24} k_{26} + \left(k_{24} + k_{26}\right)\left(P^*_{BFNPZ} + B^*_{BFNPZ} + \alpha - \gamma - \varepsilon - 1\right) + k_{24}\beta + k_{26}\delta \right]$$ (74)
$$+ k_{24} k_{26} \left(P^*_{BFNPZ} + B^*_{BFNPZ} + \alpha - \gamma - \varepsilon - 1\right) = 0$$
$$\Rightarrow N^*_{BFNPZ} = 0.4707,$$

$$P^*_{BFNPZ} = \frac{k_{19}}{k_4 \left(1 - k_{20}\right)} = 0.1667,$$ (75)

$$Z^*_{BFNPZ} = \left(\frac{k_{23}}{k_4}\right) \left(\frac{N^*_{BFNPZ}}{N^*_{BFNPZ} + k_{24}}\right) - \left(\frac{k_1}{k_4}\right) \left(\frac{B^*_{BFNPZ}}{P^*_{BFNPZ} + k_2}\right) = 0.3394,$$ (76)

where
$$\alpha = k_1 \left(1 - k_{11}\right) \left(\frac{P^*_{BFNPZ}}{P^*_{BFNPZ} + k_2}\right) \left(\frac{B^*_{BFNPZ} + k_9}{k_8}\right), \qquad \beta = k_{25} \left(1 - k_{11}\right) \left(\frac{B^*_{BFNPZ} + k_9}{k_8}\right),$$

$$\gamma = k_{10} \left(\frac{B^*_{BFNPZ} + k_9}{k_8}\right), \quad \delta = \frac{k_{23}}{k_4} \quad \text{and} \quad \varepsilon = \frac{k_1}{k_4} \left(\frac{B^*_{BFNPZ}}{P^*_{BFNPZ} + k_2}\right) \quad \text{and only the positive root is}$$

considered. The eigenvalues at this point were calculated numerically and are all found to be complex conjugates, with one pair (weakly) unstable.

Figure 2
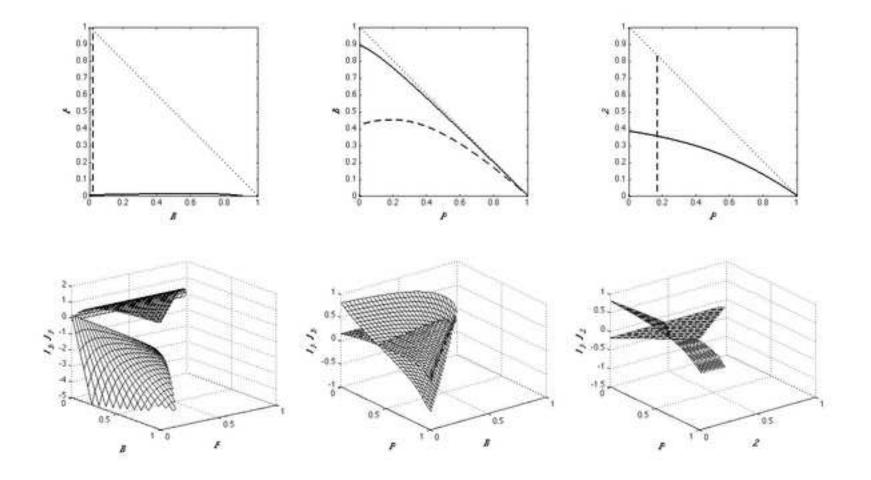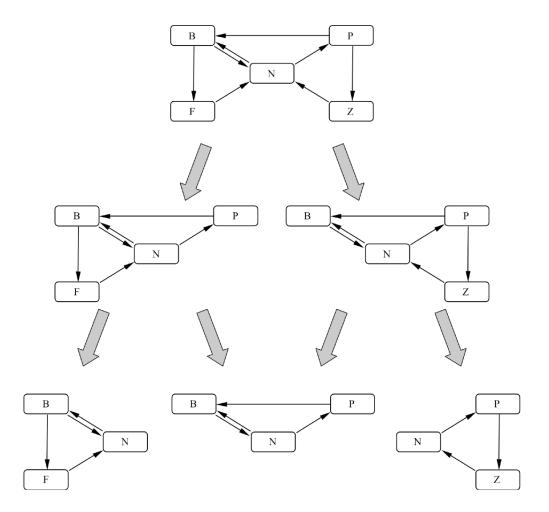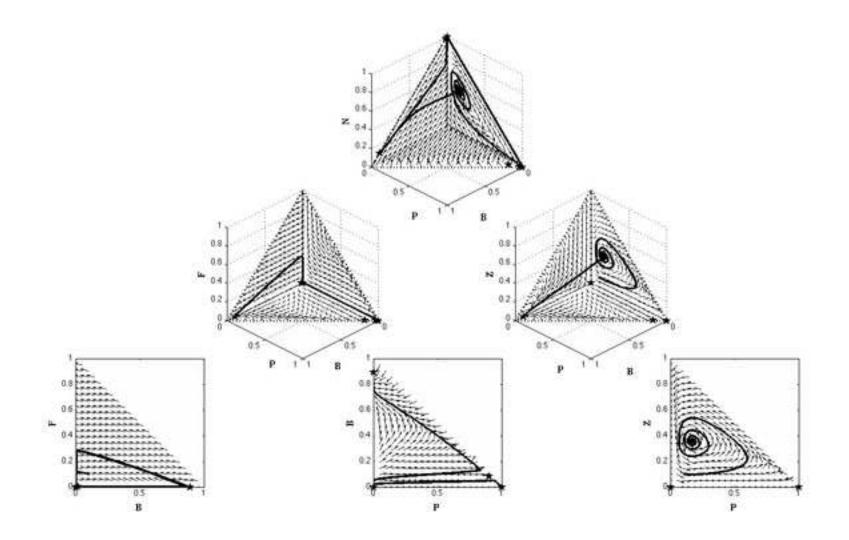
Figure 4
Click here to download high resolution image
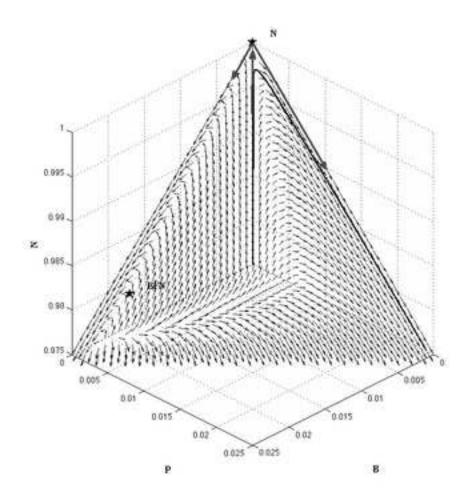
Figure 6
Click here to download high resolution image

Figure 7
Click here to download high resolution image

Figure 8
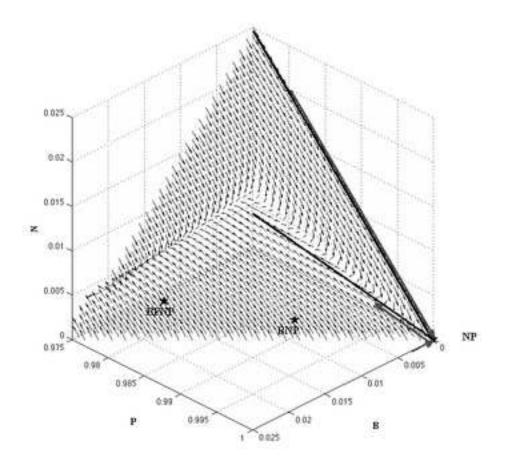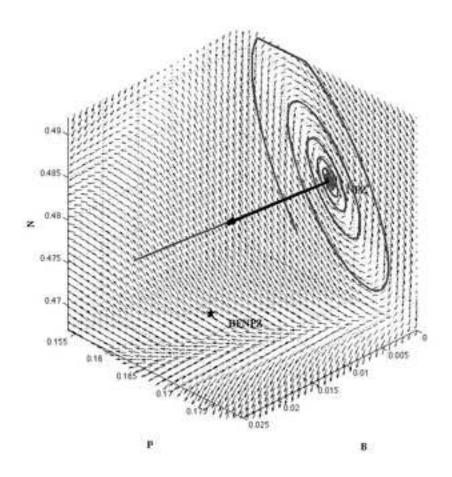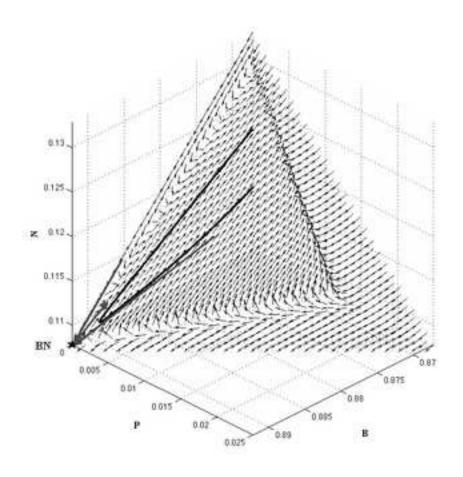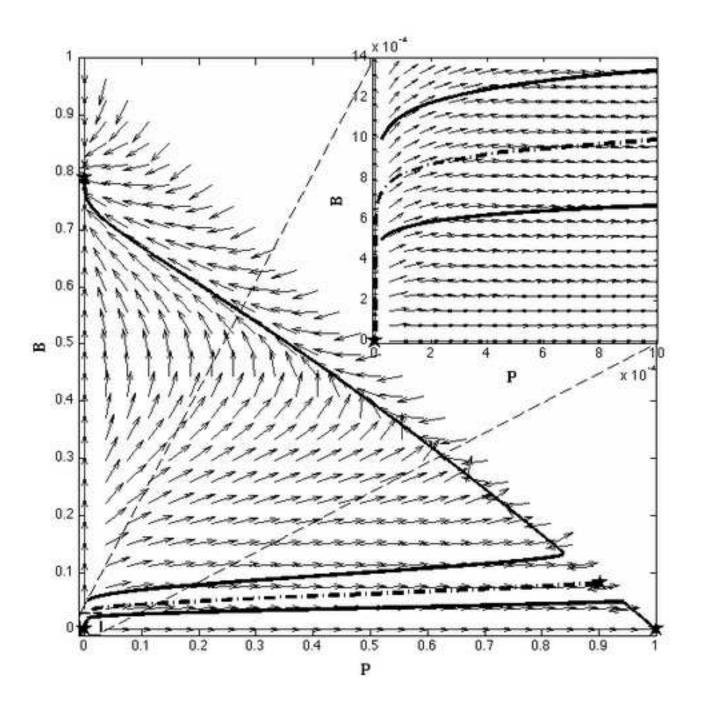**Click here to download high resolution image**